



Photokilling cancer cells using highly cell-specific antibody–TiO₂ bioconjugates and electroporation

Juan Xu^a, Yi Sun^a, Junjie Huang^a, Chunmei Chen^b, Guoyuan Liu^b,
Yan Jiang^b, Yaomin Zhao^a, Zhiyu Jiang^{a,*}

^a Department of Chemistry, Fudan University, Shanghai, China

^b Institute of Genetics, Fudan University, Shanghai, China

Received 10 February 2007; received in revised form 6 June 2007; accepted 17 June 2007

Available online 23 June 2007

Abstract

In this paper, it was reported for the first time that the combination of the electroporation and the conjugation of the TiO₂ nanoparticles with the monoclonal antibody could improve the photokilling selectivity and efficiency of photoexcited TiO₂ on cancer cells in the photodynamic therapy (PDT) because the conjugation of the TiO₂ nanoparticles with monoclonal antibodies could increase the photokilling selectivity of TiO₂ nanoparticles to cancer cells and the electroporation could accelerate the delivery speed of the TiO₂ nanoparticles to cancer cells. It was observed that using this combination method, 100% human LoVo cancer cells were photokilled within 90 min, while only 39% of the normal cells were killed under the irradiation of the ultraviolet (UV) light (365 nm). Furthermore, the combination method may be used to photokill various kinds of cancer cells only if the antibody conjugated on the TiO₂ nanoparticles is changed.

© 2007 Elsevier B.V. All rights reserved.

Keywords: Electroporation; Antibody–TiO₂ bioconjugate; MTT assay

1. Introduction

The TiO₂ nanoparticles are novel photo-effecting material with the band gap of 3.23 eV for anatase and 3.06 eV for rutile polymorph of TiO₂, respectively. Under the irradiation of UV light with the energy higher than that of the band gap of TiO₂, i.e. the light wavelength shorter than 385 and 400 nm for anatase and rutile polymorphs, respectively, the electrons in the valence band of TiO₂ can be excited to the conduction band, creating the pairs of photo-induced electron and hole [1]. These photo-induced electrons and holes present the strong reduction and oxidation properties. In the aqueous environment, the photo-induced holes can react with hydroxyl ions or water to form powerful oxidizing radicals, such as hydroxyl radicals OH[•] and perhydroxyl radicals HO₂[•] [2], which can destroy the structure of various organic molecules [3–6].

The application of TiO₂ nanoparticles in life science is attracting more and more attention since the first report of photocatalytic disinfection by Matsunaga et al. in 1985 [7]. In recent years, TiO₂ nanoparticles were applied in the field of phototherapy of malignant cells, and have been regarded as the potential photosensitizing agents for photodynamic therapy (PDT) due to their unique phototoxic effect upon the irradiation [2,8–12]. However, the TiO₂ nanoparticles still have some drawbacks in the clinical use, such as insufficient selectivity and low efficiency resulted from lack of cell-specific accumulation of TiO₂ on cancer cells. In addition, a relatively high concentration of TiO₂ nanoparticles is needed (commonly higher than 50 µg/mL). Hence, it is necessary to modify TiO₂ nanoparticles with some biomolecules that can specifically bind with cancer cells for improving selectivity and efficiency.

Recently, the high affinity and specificity of antibodies to antigens have been used to improve the performance of PDT agents [13]. For example, the monoclonal antibodies have been conjugated with some porphyrin-based photosensitizers to improve the specificity of PDT agents [14]. However, the

* Corresponding author. Tel.: +86 21 65642404; fax: +86 21 65641740.

E-mail address: zyjiang@fudan.ac.cn (Z. Jiang).

conjugation of TiO₂ nanoparticles with monoclonal antibodies has not been reported. In this study, we firstly conjugated TiO₂ nanoparticles with a specific antibody against the carcinoembryonic antigen [15] (CEA) of human LoVo cancer cells, which is useful for target accumulation of TiO₂ nanoparticles on LoVo cancer cells. Furthermore, we utilized electroporation to improve the delivery of antibody–TiO₂ bioconjugates into the cancer cells. Electroporation [16–19] is an important bioengineering technique that has been used to deliver genes or anticancer drugs into the cytoplasm through the micropores on the cell membrane produced through electric stimulation and have been successfully utilized in photodynamic therapy. In contrast to previous work, our combination method has higher cell-specificity and efficiency for photokilling cancer cells owing to the highly specific reaction between the antibody in antibody–TiO₂ conjugates and the antigen on cancer cells, which facilitated the selective accumulation of TiO₂ nanoparticles on cancer cells, and the electroporation procedure obviously increased the efficiency for photokilling LoVo cancer cells.

2. Materials and methods

2.1. Chemicals

TiO₂ (p-25, 75% anatase, 25% rutile; average diameter 25 nm, Degussa, Germany), the purified anti-CEA monoclonal antibody, Clone F6 (Everlong biotechnology Co. Ltd., Hangzhou, China), Fluorescein isothiocyanate (FITC, Sigma Co., USA), trypsin–EDTA (Invitrogen Co., USA), LoVo cells and TE353.sk cells (ATCC), MTT [3-(4, 5-dimethylthiazol-2-yl)-2, 5-diphenyltetrazolium bromide] kits (Beyotime Co. Ltd., Nantong, China), Ham's F12 medium (PAA laboratories, Australia) added with 50 µg/mL penicillin and 15% fetal calf serum (FCS), DMEM medium containing 15% FCS, L-glutamine and 50 µg/ml penicillin (Invitrogen Co., USA) were used as received. All other chemical reagents were of analytical grade. All solutions were prepared with Milli-Q water (Millipore).

2.2. Cell line

CEA-expressing cell line, LoVo (908 ng CEA per 10⁶ cells) and none-CEA-expressing cell line, TE353.sk, were employed to investigate the selective cellular uptake of antibody-conjugated TiO₂ nanoparticles. LoVo cells were grown *in vitro* in Ham's F12 medium in a humidified incubator with 5% CO₂ at 37 °C. TE353.sk cells were cultured *in vitro* in the DMEM medium.

2.3. Synthesis of FITC-antibody–TiO₂

The TiO₂ nanoparticles were ultrasonically dispersed in the phosphate buffer solution (pH 6.5) to produce the TiO₂ suspension after they were grinded in the rotating agate mortar with a small amount of ethanol at 450 r/min for 10 h. Subsequently, the TiO₂ suspension was filtrated through a 0.45 µm dialyzer after it was sterilized using an autoclave. Due to the aggregation of the TiO₂ nanoparticles, they could not be

completely sonically dispersed during sterilization. The quantity of the TiO₂ nanoparticles in the suspension was assessed using an Inductively Coupled Argon Plasma-Atomic Emission Spectrometer (ICP-AES, IRIS Intrepid, USA). The average size and the morphology of the TiO₂ nanoparticles were measured with a Transmission Electron Microscopy (TEM, JEOL JEM2011, Japan). The fluorescence emission spectra were recorded using a Cary Eclipse Fluorescence Spectrophotometer (VARIAN, USA). The UV–Vis absorption spectra were recorded using an Ultraviolet–Visible Spectrophotometer (UV, 8453, Agilent, USA).

The anti-CEA antibody was dialyzed in the carbonate buffer solution (pH 9.5) overnight. 1 mg FITC was dissolved in 1 mL dimethyl sulfoxide (DMSO) to obtain the FITC–DMSO solution. Then, after 20 µL FITC–DMSO solution was added into 1 mL 2 mg/mL anti-CEA antibody, the mixture solution was incubated at 4 °C overnight and dialyzed in the phosphate buffer solution (PBS, pH 7.4) for 16 h. The FITC-labeled monoclonal antibody (FITC-antibody) solution obtained was added into the above pH-adjusted TiO₂ suspension with the ratio of 800 µL antibody solution with 1 mg TiO₂ nanoparticles in a sterilized tube. The suspension was gently stirred at the room temperature for 1 h, followed by the incubation at 4 °C for 5 days. Finally, the conjugation of FITC-antibody and TiO₂ nanoparticles (FITC-antibody–TiO₂) was obtained by centrifuging the solution at a rate of 10000 r/min for 30 min at 4 °C. The precipitate was washed with phosphate buffer solution for three times. The FITC-antibody–TiO₂ conjugate was stored at 4 °C before use. The antibody-modified TiO₂ (antibody–TiO₂) conjugate was prepared with the similar method.

2.4. Modification of antibody–TiO₂ conjugates on cancer cell

The binding of the FITC-antibody–TiO₂ conjugate with the incubated LoVo cancer cells or TE353.sk normal cells was examined with the immunofluorescence tests. 5 × 10⁴ cells/mL LoVo cancer cells or TE353.sk normal cells were trypsinized and suspended in a low serum medium (0.05% FCS). The cells were incubated with 100 µL FITC-antibody–TiO₂ conjugate for 30 min and then were centrifuged at 1100 r/min for 6 min. The precipitated cells were suspended again in 0.3 mL phosphate buffer solution. The optical and fluorescence microscopic images of LoVo cancer cells and TE353.sk normal cells after the incubation with FITC-antibody–TiO₂ conjugates were recorded using a confocal laser scanning microscope (LEICA TCS NT, Japan). The excitation light (490 nm) was from a solid-state diode-pumped laser. A long-pass filter (515 nm) was used as emission filter for measuring the fluorescent images of samples.

2.5. Electroporation

Firstly, 5 × 10⁴ cells/mL LoVo cancer cells or TE353.sk normal cells were trypsinized, centrifuged and suspended in the culture medium. Then, 500 µL cell suspension was added into the electroporation device with a pair of flat stainless steel electrodes with 4 mm distance between two electrodes. After

the incubation of cells with 100 μL FITC-antibody–TiO₂ conjugate for 30 min, the electroporation process was carried out with the rectangular electric pulses with voltage of 500 V/cm, 100 μs duration time for 8 times with a generated Gene Pulser Xcell (Bio-RAD, USA).

2.6. Cytotoxicity test

The photokilling effect on LoVo cancer cells in different conditions was tested as follows. Firstly, LoVo cells were trypsinized and suspended in culture medium at a concentration of 5×10^4 cells/mL. Secondly, 2 mL cell suspension was added to the sterile dish. The cells adhered onto the dish wall after 24 h incubation. Thirdly, the culture medium was replaced by 1 mL antibody–TiO₂ suspension and 1 mL fresh culture medium for each dish. After incubation for 24 h, these adhered cells were washed twice with sterile phosphate buffer solution (pH 7.4). Finally, it was placed under the irradiation of UV lights with the intensities of 4 mW/cm² at wavelength of $\lambda_{\text{max}} = 253.7$ nm for a certain time. The photokilling experiment was also carried out under the irradiation of UV lights with the intensities of 1.8 mW/cm² at wavelength of $\lambda_{\text{max}} = 365$ nm. The photokilling efficiency for TE353.sk normal cells was similarly evaluated. In the cytotoxicity experiment, it is important to spray the cells as evenly as possible.

The cell viability in the culture medium was determined by MTT assay [12] using thiazoyl blue as dye and recorded with a BIO-RAD M-450 microplate reader. In the MTT assay, the absorbance of formazan produced in the cleavage of MTT by dehydrogenases in living cells at 570 nm was linearly proportional to the number of the living cells. Briefly, 250 μL of MTT solution was added into the culture dish and incubated at 37 °C for 4 h. Then, 2 mL DMSO was added into each well and mixed thoroughly to dissolve all formazan. After continuing the incubation for a few minutes at 37 °C to ensure that formazan was completely dissolved. 300 μL solutions were dispensed into the wells of 96-well plates. The plates were evaluated spectrophotometrically at 570 nm and the absorbance, $[A]_t$ was obtained. The survival fraction could be calculated according to $[A]_t/[A]_i$, where $[A]_i$ is the optical absorbance of the untreated

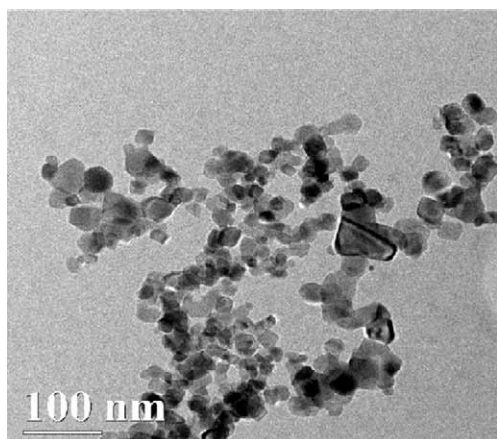


Fig. 1. TEM image of TiO₂ nanoparticles.

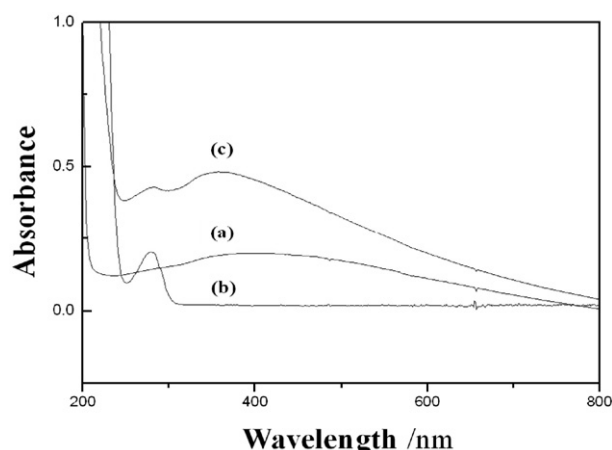


Fig. 2. UV–vis absorption spectra of (a) TiO₂ suspension; (b) antibody solution; (c) anti-CEA antibody coated TiO₂ suspension.

cells. 4-fold replicates were carried out per drug and dose and each experiment was repeated three times with S.D. = $\pm 4\%$ for each determination. The variation region and the average value of the resulting data are presented in the resulting diagrams.

3. Results and discussion

3.1. Cancer cells modified by antibody–nano-TiO₂ conjugates

The TEM image of TiO₂ particles is presented in Fig. 1. As can be seen, most of the TiO₂ particles were spherical or square-shaped with the particle size of 15–35 nm.

The conjugation of the FITC-antibody–TiO₂ nanoparticles was checked by UV–Vis absorption spectrum and fluorescence emission spectra. Fig. 2 shows the UV–Vis absorption spectra of the TiO₂ suspension, antibody solution and antibody–TiO₂ suspension. It can be observed a broad absorption peak at about 390 nm in the spectrum of the TiO₂ suspension (Fig. 2, curve a) and an absorption peak at 280 nm in the spectrum of the antibody solution (Fig. 2, curve b). In the spectrum of antibody–TiO₂ suspension, two absorption peaks are located at 360 and 285 nm (Fig. 2, Curve c). It indicated that in the spectrum of antibody–TiO₂ suspension, the absorption peak of TiO₂ shifts from 390 to 360 nm and the absorption peak of antibody shifts from 280 to 285 nm. This demonstrated that antibody has been immobilized on the surface of TiO₂ nanoparticles.

Fig. 3 shows the fluorescence emission spectra of the suspension of TiO₂ nanoparticles, the FITC-antibody solution and the suspension of FITC-antibody–TiO₂ conjugate. It was observed from Fig. 3 that the TiO₂ nanoparticles have no fluorescence emission when excited at 490 nm (Fig. 3, Curve a) and the FITC-antibody exhibits a fluorescence emission peak at about 515 nm (Fig. 3, Curve b). For FITC-antibody–TiO₂ conjugate suspension, a broader and weaker peak appears at about 510 nm (Fig. 3, Curve c), reflecting the existence of antibody on the TiO₂ nanoparticles. The shift in the peak position is not large because the fluorescence peak is due to FITC. This may illustrate that not FITC, but the antibody is attached to the surface of the TiO₂ nanoparticles.

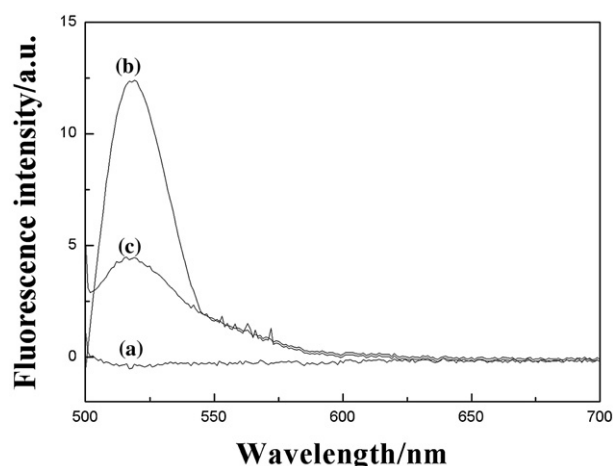


Fig. 3. The fluorescence emission spectra of (a) the suspension of the TiO_2 nanoparticles; (b) the FITC-labeled antibody solution; (c) the suspension of FITC-antibody- TiO_2 conjugate. Wavelength of the excitation light: 490 nm. The concentration of TiO_2 : 3.12 $\mu\text{g}/\text{mL}$.

Fig. 4 displays the optical and fluorescence microscopic images of the LoVo cancer cells and TE353.sk normal cells after the incubation in the culture medium. It was observed from Fig. 4 that after the incubation in the culture medium containing the FITC-antibody- TiO_2 conjugate for 30 minutes, LoVo cancer cells clearly exhibit the green fluorescence light (Fig. 4A), but TE353.sk normal cells do not show any fluorescence (Fig. 4B),

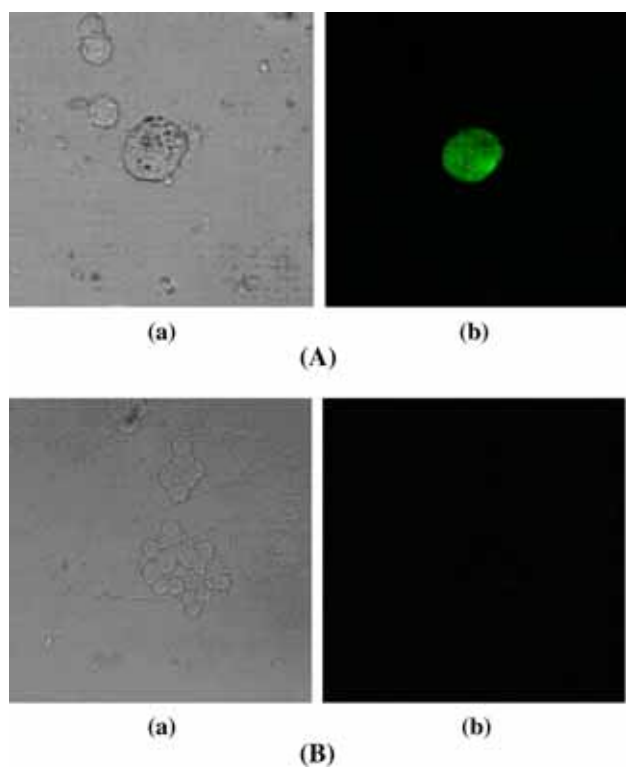


Fig. 4. (a) The optical and (b) fluorescence microscopic images of (A) LoVo cancer cells and (B) TE353.sk normal cells after the incubation in the culture medium containing 3.12 $\mu\text{g}/\text{mL}$ FITC-antibody- TiO_2 conjugates for 30 min.

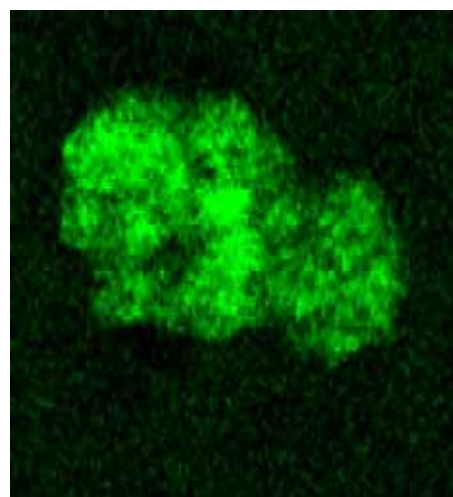


Fig. 5. The fluorescence microscopic image of the LoVo cancer cells after the incubation in the culture medium containing 3.12 $\mu\text{g}/\text{mL}$ FITC-antibody- TiO_2 conjugate and then the electroporation with the electric pulses at 500 V/cm for 100 μs .

indicating that the FITC-antibody- TiO_2 conjugate has attached to the LoVo cancer cells, but does not attach to the TE353.sk cells due to the specific reaction between antibody in the FITC-antibody- TiO_2 bioconjugates and antigen of the LoVo cancer cells. This illustrated that the FITC-antibody- TiO_2 conjugate possesses good selectivity.

Fig. 5 shows the fluorescence microscopic image of the LoVo cancer cells, which were firstly incubated in the medium containing FITC-antibody- TiO_2 conjugates for 30 min and then were suffered an electroporation treatment with voltage of 500 V/cm for 100 μs . It can be seen from Fig. 5 that the LoVo cancer cells shows much brighter green fluorescence light than

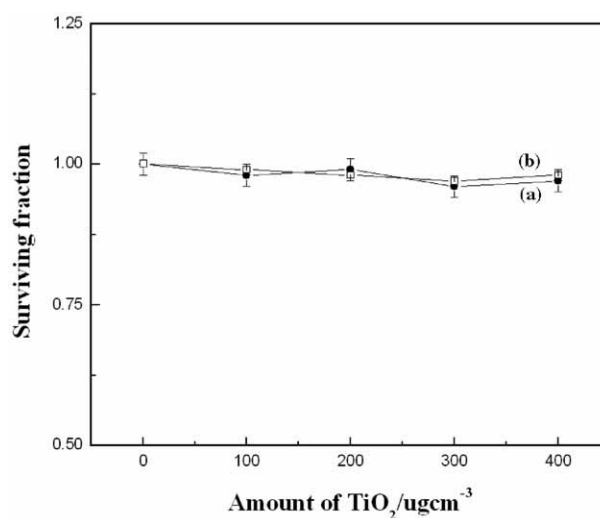


Fig. 6. The plots of the surviving fraction of (A) the LoVo cells and (B) the TE353.sk cells vs the concentration of the FITC-antibody- TiO_2 conjugate after the LoVo cells and the TE353.sk cells in culture medium were treated for 24 h in the dark, respectively.

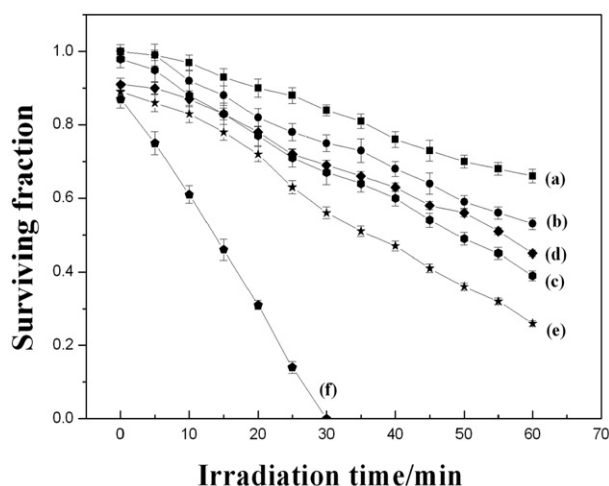


Fig. 7. The plots of the surviving fraction of the LoVo cells vs the irradiation time under the UV light after the LoVo cells were treated with (a) the UV light alone; (b) the incubation in the culture medium containing 3.12 $\mu\text{g/mL}$ TiO_2 nanoparticles; (c) the incubation in culture medium containing 3.12 $\mu\text{g/mL}$ antibody– TiO_2 conjugate, (d) the electroporation with 8 electric pulses at 500 V/cm for 100 μs ; (e) the treatment with the procedures of (b) and (d); (f) the treatment with the procedures of (c) and (d). Light wavelength: 253.7 nm, light intensity: 4 mW/cm^2 .

that in Fig. 4A. This suggested that after the electroporation, the amount of the FITC-antibody– TiO_2 conjugate entered into the LoVo cancer cells is larger than that without the electroporation because the electroporation can produce the micropores on the cell membrane.

3.2. Photokilling efficiency on LoVo cells by various treatments

Fig. 6 shows the plots of the surviving fraction of the LoVo cells and the TE353.sk cells vs the concentration of the antibody– TiO_2 conjugate after the LoVo cells and the TE353.sk cells were treated with different amounts of antibody– TiO_2 suspension for 24 h in the dark, respectively. The surviving fractions of the LoVo cells and the TE353.sk cells are almost the same. They are larger than 90% when the concentration of TiO_2 was in the range of 0–400 $\mu\text{g/mL}$. The result confirms that the FITC-antibody– TiO_2 conjugate are not toxic for both the LoVo cancer cells and the TE353.sk normal cells without the irradiation. The results are consistent with that in the previous reports [8,11,12].

Fig. 7 displays the plots of the surviving fraction of the LoVo cells vs the irradiation time under the UV light after the LoVo cells were treated under the different conditions. It was found from Fig. 7 that when the LoVo cell in the culture medium is only irradiated with the UV light and no any TiO_2 nanoparticles in the culture medium, the surviving fraction of LoVo cells at 30 min is 84% (Fig. 7, curve a). The surviving fraction of LoVo cells at 30 min is 75% when the LoVo cell in the culture medium is irradiated with the UV light and 3.12 $\mu\text{g/mL}$ TiO_2 nanoparticles exist in the culture medium (Fig. 7, curve b), indicating that the TiO_2 nanoparticles is helpful for killing the LoVo cells. If the TiO_2 nanoparticles are replaced with the

antibody– TiO_2 conjugate, the surviving fraction at 30 min is decreased to 67% (Fig. 7, curve c). After the electroporation is used and then the culture medium is irradiated with the UV light, the surviving fraction of LoVo cells at 30 min is 69% (Fig. 7, curve d), which is similar to that of only adding the antibody– TiO_2 conjugate, illustrating that the electroporation would also affect the surviving fraction of LoVo cells. The surviving fraction can be further reduced to 56% (Fig. 7, curve e) when the TiO_2 nanoparticles, the electroporation and the UV irradiation are used together. The most effective approach to kill the LoVo cells was observed when the antibody– TiO_2 conjugate, the electroporation, and the UV irradiation are combined together. Under the above conditions, the LoVo cancer cells would be completely killed after the irradiation for 30 min and the surviving fraction becomes 0% (Fig. 7, Curve f), which is 56% lower than that in Fig. 7, Curve e. Firstly, all the above results illustrated that the antibody– TiO_2 conjugate is more effective for killing the LoVo cancer cells because the antibody– TiO_2 conjugate can be accumulated on the membrane of the LoVo cells due to the specific reaction between antibody in the antibody– TiO_2 conjugate and antigen on the cell membrane. Secondly, the electroporation can promote the delivery of the antibody– TiO_2 conjugate into cells, so that the efficiency of killing the LoVo cells would be increased. Finally, it should be noticed that the concentration of antibody– TiO_2 conjugate is only as low as 3.12 $\mu\text{g/mL}$, while the concentration of the TiO_2 nanoparticles is as high as 50 $\mu\text{g/mL}$ for completely killing the cancer cells when the TiO_2 nanoparticles was used and the electroporation technique is not applied [9].

Fig. 8 compares the surviving fractions of the LoVo cancer cells and TE353.sk normal cells under the identical conditions. It can be observed from Fig. 8 that after 90 min, only 39% TE353.sk cells are killed and all the LoVo cells are killed. This illustrated that as expected, the antibody– TiO_2 conjugate possesses the high cell-specificity and thus, the efficiency for photokilling LoVo cancer cells is high.

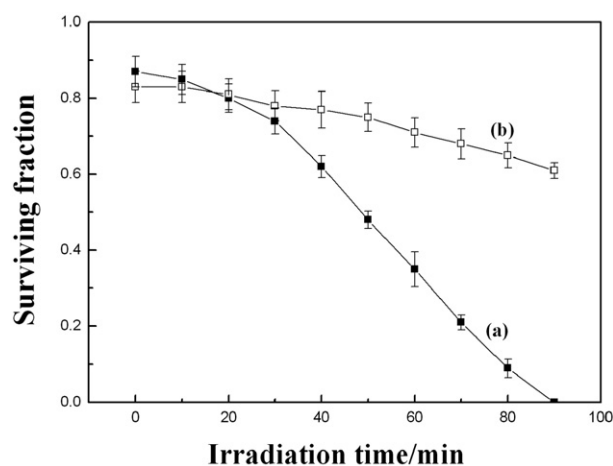


Fig. 8. The plots of the surviving fraction vs the irradiation time under the UV light with the wavelength of 365 nm and intensity of 1.8 mW/cm^2 for (a) the LoVo cells and (b) the TE353.sk cells in the presence of the antibody– TiO_2 conjugate and after the electroporation treatment.

4. Conclusions

In summary, in this paper, a novel method combined the antibody–TiO₂ conjugate with the electroporation was suggested. This method showed a high efficiency and cell-specificity for photokilling LoVo cancer cells in the case of using very low concentration of antibody–TiO₂ bioconjugate (3.12 µg/mL). This new method also has the advantage that it might be used to kill various kinds of cancer cells with changing the type of antibody. This approach may be used to produce targeted cytotoxicity and explored as a novel photodynamic therapy for cancers in the future.

References

- [1] T. Ashikaga, M. Wada, H. Kobayashi, M. Mori, Y. Katsumura, H. Fukui, S. Kato, M. Yamaguchi, T. Takamatsu, Effect of the photocatalytic activity of TiO₂ on plasmid DNA, *Mutat. Res.* 466 (2000) 1–7.
- [2] A. Fujishima, T.N. Rao, D.A. Tryk, Titanium dioxide photocatalysis, *J. photochem. Photobiol. C* 1 (2000) 1–21.
- [3] O.A. Semenikhin, V.E. Kazarinov, L. Jiang, K. Hashimoto, A. Fujishima, Suppression of surface recombination on TiO₂ anatase photocatalysts in aqueous solutions containing alcohol, *Langmuir* 15 (1999) 3731–3737.
- [4] S. Fukahori, H. Ichiura, T. Kitaoka, H. Tanaka, Capturing of bisphenol A photodecomposition intermediates by composite TiO₂–zeolite sheets, *Appl. Catal., B Environ.* 46 (2003) 453–462.
- [5] C.H. Wu, K.S. Huang, J.M. Chern, Decomposition of acid dye by TiO₂ thin films prepared by the sol–gel method, *Ind. Eng. Chem. Res.* 45 (2006) 2040–2045.
- [6] M.A. Henderson, Complexity in the decomposition of formic acid on the TiO₂(110) surface, *J. Phys. Chem., B* 101 (1997) 221–229.
- [7] T. Matsunaga, R. Tomoda, T. Nakajima, et al., Photoelectrochemical sterilization of microbial cells by semiconductor powders, *FEMS Microbiol. Lett.* 29 (1985) 211–214.
- [8] R.X. Cai, K. Hashimoto, K. Itoh, et al., Photokilling of malignant cells with ultrafine TiO₂ powder, *Bull. Chem. Soc. Jpn.*, 64 (1991) 1268–1273.
- [9] H. Sakai, E. Ito, R.X. Cai, et al., Intracellular Ca²⁺ concentration change of T24 cell under irradiation in the presence of TiO₂ ultrafine particles, *Biochim. Biophys. Acta* 1201 (1994) 259–265.
- [10] W.G. Wamer, J.J. Yin, R.R. Wei, Oxidative damage to nucleic acids photosensitized by titanium dioxide, *Free Radic. Biol. Med.* 23 (1997) 851–858.
- [11] R. Cai, Y. Kubota, T. Shuin, et al., Induction of cytotoxicity by photoexcited TiO₂ particles, *Cancer Res.*, 52 (1992) 2346–2348.
- [12] A.P. Zhang, Y.P. Sun, Photocatalytic killing effect of TiO₂ nanoparticles on Ls-174-t human colon carcinoma cells, *World J. Gastroenterol.* 10 (2004) 3191–3193.
- [13] M. Takahashi, A. Ueno, T. Uda, H. Mihara, Design of novel porphyrin-binding peptides based on antibody CDR, *Bioorg. Med. Chem. Lett.* 8 (1998) 2023–2026.
- [14] G. Liang, L. Wang, Z. Yang, H. Koon, N. Mak, C.K. Chang, B. Xu, Using enzymatic reactions to enhance the photodynamic therapy effect of porphyrin dityrosine phosphates, *Chem. Commun.* 48 (2006) 5021–5023.
- [15] L.J.F. Hefta, M. Neumaier, J.E. Shively, Kinetic and affinity constants of epitope specific anti-carcinoembryonic antigen (CEA) monoclonal antibodies for CEA and engineered CEA domain constructs, *Immunotechnology* 4 (1998) 49–57.
- [16] J. Labanauskiene, J. Gehl, J. Didziapetriene, Evaluation of cytotoxic effect of photodynamic therapy in combination with electroporation in vitro, *Bioelectrochemistry*, 70 (2007) 78–82.
- [17] M.F. Underhill, C. Coley, J.R. Birch, A. Findlay, R. Kallmeier, C.G. Proud, D.C. James, Engineering mRNA translation initiation to enhance transient gene expression in Chinese hamster ovary cells, *Biotechnol. Prog.* 19 (2003) 121–129.
- [18] K. Nolkranz, C. Farre, K.J. Hurtig, P. Rylander, O. Orwar, Functional screening of intracellular proteins in single cells and in patterned cell arrays using electroporation, *Anal. Chem.* 74 (2002) 4300–4305.
- [19] M. Lambreva, B. Glück, M. Radeva, H. Berg, Electroporation of cell membranes supporting penetration of photodynamic active macromolecular chromophore dextrans, *Bioelectrochemistry* 62 (2004) 95–98.